Published in final edited form as:
Biochemistry. 2006 May 16; 45(19): 6003–6011. doi:10.1021/bi052247k.

Purification and spectroscopic characterization of Ctb, a group III truncated hemoglobin implicated in oxygen metabolism in the food-borne pathogen *Campylobacter jejuni*†

Laura M. Wainwright‡, **Yinghua Wang**§, **Simon F. Park**¶, **Syun-Ru Yeh**§, and **Robert K. Poole**‡,*

‡*Department of Molecular Biology and Biotechnology, The University of Sheffield, Sheffield S10 2TN, UK*

§*Department of Physiology and Biophysics, Albert Einstein College of Medicine, Bronx, NY 10461, US*

¶*School of Biomedical and Molecular Sciences, University of Surrey, Guildford GU2 7XH, UK*

Abstract

Campylobacter jejuni is a foodborne bacterial pathogen that possesses two distinct hemoglobins, encoded by the *ctb* and *cgb* genes. The former codes for a truncated hemoglobin (Ctb) in group III, an assemblage of uncharacterized globins in diverse clinically- and technologically-significant bacteria. Here, we show that Ctb purifies as a monomeric, predominantly oxygenated species. Optical spectra of ferric, ferrous, O_2- and CO-bound forms resemble those of other hemoglobins. However, resonance Raman analysis shows Ctb to have an atypical $\nu_{Fe\text{-}CO}$ stretching mode at 514 cm^{-1}, compared to the other truncated hemoglobins that have been characterized so far. This implies unique roles in ligand stabilisation for TyrB10, HisE7 and TrpG8, residues highly conserved within group III truncated hemoglobins. Since *C. jejuni* is a microaerophile, and a *ctb* mutant exhibits O_2-dependent growth defects, one of the hypothesised roles of Ctb is in the detoxification, sequestration or transfer of O_2 The midpoint potential (E_h) of Ctb was found to be −33 mV, but no evidence was obtained *in vitro* to support the hypothesis that Ctb is reducible by NADH or NADPH. This truncated hemoglobin may function in the facilitation of O_2 transfer to one of the terminal oxidases of *C. jejuni* or instead facilitate O_2 transfer to Cgb for NO detoxification.

In the past three decades, our understanding of hemoglobins has grown to recognise new classes of proteins in addition to the classical vertebrate α- and β-globins, myoglobin and the symbiotic Hbs of leguminous plants. These 'new' globins - some of which may actually be amongst the oldest, or ancestral, globins in a phylogenetic context (1) - include the non-symbiotic plant Hbs, chimeric flavohemoglobins, and the trHbs. Globins may be classified functionally - into those that detoxify NO and those that are involved in O_2 transfer or detoxification – or structurally into three categories (2). The first structural category contains flavoHbs that possess a C-terminal ferredoxin-$NADP^+$ reductase-like domain and an N-terminal globin domain; bacterial (3,4) and yeast (5) examples function in the enzymic removal of NO to produce nitrate (6,7). The second category contains single domain Hbs that are very similar to the N-terminal domain of the flavoHbs; however, their functions appear more varied than those of the flavoHbs. As an example, Vgb, found in the obligate aerobe *Vitreoscilla*, is believed to function in the facilitation of O_2 transfer to cytochrome *bo'* (8), whereas the *C. jejuni* Hb, Cgb,

†This work was supported by the Biotechnology and Biological Sciences Research Council (BBSRC, UK) through Research Grant D18084 and the National Institutes of Health through NIH Grant HL65465.

*To whom correspondence should be addressed. Phone: (+44) 114 222 4447. Fax: (+44) 114 222 2800. E-mail: r.poole@sheffield.ac.uk.

confers tolerance to NO (9) and is up-regulated by NO and its congeners by an NO-activated transcriptional regulator (10).

The trHbs comprise the third category: members possess an altered structure whereby the globin fold is edited from the three-over-three α-helical sandwich (3/3) characteristic of vertebrate globins to a two-over-two arrangement (11) and are thus sometimes called 2/2 Hbs (1). This results in a considerably smaller globin composed typically of 110-130 amino acids. A subdivision of the trHbs, based on the information available from more than 40 actual or putative trHb genes, was proposed by Wittenberg *et al*. (12). Three distinct groups were identified (I, II, III), with four subgroups occurring within group II. Few amino acids are strictly conserved throughout the trHb sequences, only the proximal HisF8 being invariant (see below). Note that we use here the terms group I, II and III in this context as defined by Wittenberg *et al.* (12) and not to distinguish between the truncated globins, myoglobin-like proteins and flavohemoglobins (13).

The crystal structures of trHbs from *Chlamydomonas*, *Paramecium* (11), *M. tuberculosis* (14,15) and *Synechocystis* (16) have been solved. The antiparallel helix pairs are comprised of B/E and G/H. The A helix is almost entirely deleted, the instability implied by this absence being remedied by the presence of a hydrophobic amino acid cluster in the AB region to allow efficient sealing of the proximal side of the heme pocket (11). There are three conserved Gly-Gly motifs located in, respectively, the AB hinge (11), the EF hinge and at the end of the pre-F loop (17) that are believed to stabilise the globin fold. Only group I and II trHbs possess the Gly-Gly motifs; little is known concerning the putative motifs that replace them in terms of stabilisation within group III. The F helix is attenuated to a single turn, the rest being replaced by an extended polypeptide segment termed the pre-F loop (11). Group II trHbs have a conserved EF loop, whereas this area in group I trHbs is shorter and lacking sequence conservation (18). The C helix is barely present and the CD-D region is reduced to approximately three residues, arguably the smallest polypeptide span that could join the C and E helices (12).

There are only a few strictly conserved residues within the known trHb sequences. The trHbs without exception retain the conserved HisF8 residue as the proximal ligand to the heme. However, the conserved residues of the distal pocket are more variable. At the B9-B10 sites, there is a strongly conserved Phe-Tyr couplet, the TyrB10 being involved in heme ligand stabilisation (12). Position CD1 is conserved as Phe in group I and III trHbs; those residues in group II inhabiting the position can be Phe, Tyr or His. The E7 position is more variable: in group I trHbs the position is occupied mostly by GlnE7, group III trHbs invariably have HisE7, and in group II Ala, Ser or Thr can occupy this position. Phe almost always occupies the E14 position in all groups; this residue is believed to shield the heme from solvent in a role comparable to that of PheCD1 in other hemoglobins (12).

The gram-negative microaerophilic bacterium *Campylobacter jejuni* is notable but not unique in possessing two different Hbs. In addition to Cgb, a single-domain (3/3) Hb (9), it possesses Ctb (19) that belongs to trHb group III. This is by far the least well-understood family of Hbs, despite the fact that it embraces globins (12) from the pathogens *Bordatella pertussis* and *Mycobacterium avium* and the obligately aerobic metal-leaching acidophilic bacterium *Thiobacillus ferrooxidans. C. jejuni* is now recognised as one of the most important causes of bacterial gastroenteritis worldwide (20). In humans, campylobacteriosis is mainly a food-borne disease. However, *C. jejuni* is commonly a gut commensal in many food-producing animals and birds and contamination of meat during processing is an important method of transfer (20). Cgb protects the bacterium from the toxic effects of NO (9), but the group III trHb has no clearly defined function. Its expression is, however, elevated in response to nitrosative stress, a response mediated by the NssR sensor/regulator (10). The microaerophilic nature of

C. jejuni implies the presence of mechanisms for high affinity O_2 binding and/or coping with O_2 toxicity and it is possible that Ctb fulfils one of these functions (19). In the present work, we have cloned and over-expressed the *C. jejuni* Ctb (Cj0465c), characterized it through optical and resonance Raman spectroscopy, and determined its mid-point redox potential. This is the first detailed characterization of a group III trHb.

EXPERIMENTAL PROCEDURES

Bacterial strains and culture conditions

Campylobacter jejuni strain NCTC 11168 was obtained from the National Collection of Type Cultures (London). *E. coli* TOP10 (Invitrogen) was used for the overexpression of Ctb; the expressing strain was named RKP4979. *C. jejuni* strains were grown at 42 °C in Mueller-Hinton medium in a modular atmosphere controlled system (MACS) VA500 workstation (Don Whitley Scientific) with a constant gas supply of 10 % oxygen, 10 % carbon dioxide and 80 % nitrogen. Plates were incubated for 48 h; cells from these were inoculated into 50 ml of liquid culture in a 100 ml flask and grown for approximately 18 h. The apparent absorbance (OD_{600}) was adjusted to 0.5 and cultures reinoculated at 1.33 % (v/v) into fresh medium in 250 ml baffled flasks, then grown with shaking at 115 rpm. Mueller-Hinton medium was supplemented with vancomycin (10 μg/ml). *E. coli* strains were grown in Luria-Bertani (LB) medium at 37 °C at 200 rpm, and on nutrient agar at the same temperature. The media were supplemented with ampicillin (50 μg/ml).

Cloning and expression of C. jejuni trHb in E. coli

Genomic DNA was isolated from *C. jejuni* NCTC 11168 using guanidium thiocyanate (21). The forward (RP268, 5' AAAATTAACATTTAACCATGGCTTATA TG AAATTTGAAAC-3') and reverse (RP267, 5'-GAAAAGGTAAAAAAAGC TTTGGCAAAAAAATTG-3') primers were designed based on the sequence of the *C. jejuni* genome and contained an *Nco*I and *Hin*dIII site respectively (underlined). PCR products were visualised on a gel. The 0.38 kb fragment was recovered with a Qiaquick gel extraction kit (Qiagen), cloned between the *Nco*I and *Hin*dIII sites of pBAD/His (Invitrogen) and transformed into *E. coli* TOP10 using the method of Inoue *et al*. (22) The construct was checked by sequencing from just upstream of the promoter through to the end of the insert. For the overexpression, starter cultures grown overnight in LB supplemented with ampicillin were inoculated at 1 % (v/v) into 500 ml LB in 2 L baffled flasks supplemented with ampicillin, 200 μM δ-aminolevulinic acid, and 12 μM $FeCl_3$. The cultures were shaken at 200 rpm until an OD_{600} of ~ 0.5 had been reached; they were then induced with 0.02% arabinose and grown for a further 4 h. Concentrations of δ-aminolevulinic acid, $FeCl_3$ and arabinose were selected after preliminary optimisation studies.

Purification of C. jejuni trHb

All buffers used in purification were made up using MilliQ water. Commonly, 4 L of culture were grown for a single purification. The cells were harvested by centrifugation at 5000 × g for 10 min at 4 °C and resuspended in 80 ml of 50 mM Tris-HCl (pH 7.0). Cells were broken by ultrasonication and cell debris removed by centrifugation at 21000 × g for 15 min at 4 °C. The clear supernatant obtained was reddish brown in colour and was loaded onto a 30 ml DEAE Sepharose Fast Flow (Pharmacia Biotech) column equilibrated with 50 mM Tris-HCl (pH 7.0) in an Åkta Purifier (GE Healthcare Bio-Sciences, Amersham Biosciences UK Ltd). The column was washed with 40 ml of the same buffer and the trHb eluted with a NaCl gradient (from 0 to 0.5 M) in 50 mM Tris-HCl buffer (pH 7.0). Fractions to be carried forward for the next step were chosen on the basis of coincidence of the heme (412 nm) and protein (280 nm) peaks in the UV-visible absorption profile. The eluate was concentrated to ~1.4 ml using a Vivaspin 20 concentrator (Vivascience) with a molecular mass cut-off of 5 kDa. This fraction was further

purified by gel filtration. A Superdex-200 column (16 × 60 cm, GE Healthcare Bio-Sciences, Amersham Biosciences UK Ltd) was equilibrated with 50 mM Tris-HCl (pH 7.0) containing 0.2 M NaCl. A 1 ml portion of the previous fraction was applied and eluted in the equilibration buffer at a flow rate of 1 ml/min. Pure Ctb was stored at 4 °C.

O_2 consumption studies

A digital Clark-type electrode system (Model 10: Rank Brothers) connected to a chart recorder was used to measure O_2 consumption. Experiments were carried out at 37 °C in a 1.5 ml volume. Na dithionite and air-saturated buffer were used to calibrate the electrode and experiments with 3.3 to 9.5 μM Ctb (final concentrations) were performed in 50 mM K phosphate buffer (pH 7.0). Additions of experimental components were made through the lid with a Hamilton syringe. The pure Ctb used was in the oxygenated form.

Visible absorbance spectroscopy

Absorption spectra were recorded using a custom-built SDB4 dual wavelength scanning spectrophotometer (University of Pennsylvania School of Medicine Biomedical Instrumentation Group and Current Designs, Philadelphia, PA) as described by Kalnenieks *et al.* (23). Ctb was reduced using a few grains of Na dithionite. CO binding was achieved by bubbling reduced samples for 2 min with the gas. Samples were oxygenated by passage of reduced globin down a Sephadex G-25 column (Amersham Biosciences) in aerated 50 mM Tris-HCl pH 7.0. Ctb was oxidised using K ferricyanide or ammonium persulfate.

Measurement of redox potential

This was carried out at room temperature in the previously described dual wavelength spectrophotometer according to the method of Dutton (24) in a custom-built cuvette of 10 mm pathlength. A ThermoRussell CMMPtR4 Ag/AgCl redox electrode was used (4 M KCl electrolyte). It was calibrated against a solution of 0.1 M K ferrocyanide and 0.05 M K ferricyanide. Oxidised Ctb was obtained by dialysis of the pure protein against 4 L of 50 mM glycine HCl buffer (pH 2.5) at 4 °C overnight with stirring. Ferric Ctb was then dialysed back into 50 mM Tris HCl pH 7.0 and used at 9 μM (final concentration) in 50 mM MOPS buffer (pH 7.0) for the titration. The following redox mediators at the final concentrations (μM) given in parentheses were used: quinhydrone (50); *N, N, N,' N'*-tetramethylene-*p*-phenyldiamine (20); 1,2-naphthoquinone-4-sulphonate (40); naphthoquinone (25); trimethylhydroquinone (20); phenazine methosulfate (12.5); phenazine ethosulfate (20); 1-methyl-1,4-naphthoquinone (20); 1-hydroxy-1,4-naphthoquinone (25). Ctb was progressively reduced by titration with an anoxic Na dithionite solution, and spectra were recorded approximately every 20 mV. The ΔA (432-452.5 nm) was measured. Reverse titrations were performed with a K ferricyanide solution. The midpoint potential was determined by plotting redox potential against % oxidised Ctb/ % reduced Ctb. The midpoint potential was taken to be the poise at which % oxidized/ % reduced equals 1 (24).

Resonance Raman techniques

The concentration of protein samples used for the Raman measurements was typically 30-100 μM in phosphate-buffered saline. Raman measurements with Soret excitation were taken with previously described instrumentation (13,25,26). Briefly, the 413.2 nm line of a krypton ion laser (Spectra Physics, Mountain View, CA) was used as an excitation source. The laser power was maintained in the 0.5-2 mW range to minimise CO dissociation. The Raman scattered light was dispersed through a polychromator (Spex, Metuchen, NJ) equipped with a 1200 grooves/mm grating and detected by a liquid nitrogen-cooled CCD camera (Princeton Instruments, Princeton, NJ). A holographic notch filter (Kaiser, Ann Arbor, MI) was used to remove the laser scattering. Typically, several 10 s (or 1 min) spectra were recorded and averaged after

removal of cosmic ray spikes by a standard software routine (CCD spectrometric multichannel analysis, Princeton Instruments, NJ). Frequency shifts in the Raman spectra were calibrated using indene as the reference. The accuracy of the spectra was approximately ±1 cm^{-1} for absolute shifts and less than ±0.25 cm^{-1} for relative shifts.

RESULTS

Sequence analyses

The *C. jejuni* trHb (accession number Cj0465c) is encoded by an approximately 0.38 kb stretch of DNA. The surrounding DNA encodes an ATP-dependent DNA helicase, a zinc protease-like protein, an ABC transporter and a regulator (NssR) - believed to be a distant member of the Crp/Fnr family - that up-regulates both Ctb and Cgb in response to nitrosative stress (10).

Fig. 1 shows a structure-based alignment of Ctb with several other microbial Hbs. The first eight Hbs are categorised as members of the trHb-III group (12) by the highly conserved PheB9, TyrB10, PheCD1, HisE7, PheE14 and HisF8. The TrpG8 is also highly conserved in members of group III. In group II trHbs, for instance the trHbO from *Mycobacterium tuberculosis*, this residue is part of a hydrogen bonding network with TyrCD1 that stabilises heme-bound ligands (13,15). Such an interaction is not possible in the *C. jejuni* trHb as the CD1 position is filled by an apolar residue (Phe). The E11 residue is conserved in group III trHbs as leucine or isoleucine. In trHbs of group II, for instance trHbN from *Mycobacterium tuberculosis* and the trHb from *Chlamydomonas eugametos*, this position is occupied by a polar residue, which is involved in the formation of a hydrogen bonding network with heme-bound ligands (11,13, 14).

Optical spectra

The *ctb* gene was cloned into pBAD and over-expressed in *E. coli*. Ctb was purified using ion exchange and gel filtration chromatography. The globin eluted from the gel filtration column as a monomer. SDS-PAGE analysis gave an estimated molecular mass of 14 kDa. This is consistent with the theoretical value of 14.06 kDa based on the amino acid composition of the protein. The absolute electronic absorbance spectra of Ctb are displayed in Fig. 2. The trHb was found as a mixture of the ferric and oxy forms when isolated (native form). It was characterized by a Soret peak at 411 nm, a broad peak at around 512 nm, a charge transfer band at 640 nm, and two peaks at 542 and 578 nm. In a typical Hb, the ferric heme iron in the resting state is axially coordinated by an exogenous water ligand in the distal position. Because water is a weak field ligand, the heme iron typically exhibits a mixture of six-coordinate high-spin and low-spin configurations. At high pH, the heme-bound water is partially deprotonated, and the contribution from the low-spin component increases, due to hydroxide being a strong field ligand for the heme iron. The 512 and 640 nm absorption bands found in Ctb are characteristic for a water-bound form with six-coordinate high-spin configuration; the 542 and 578 nm bands signal the low-spin configuration. However, the latter two bands are similar to those of the oxy form (see below). The intensity of these two bands decreased when native Ctb is exposed to an oxidant (K ferricyanide or ammonium persulfate). This oxy component is stable, decaying only gradually over a period of months at 4 °C to a predominantly ferric state.

Pure ferric species was obtained by ferricyanide oxidation under anaerobic conditions and purification using a desalting column. The species exhibits a Soret band at 410 nm and the two pairs of bands at 512 and 640 nm, and 542 and 582 nm. The ferric species can be slowly reduced by dithionite over a period of ~15 min. The reduced protein displayed a Soret band at 432 nm and a broad αβ-band with a maximum at 565 nm. Addition of carbon monoxide to the reduced form readily resulted in formation of the carbonmonoxyferroheme. This displayed a narrow Soret band at 421 nm and α-β bands at 538 and 569 nm, separated by a shallow trough. The

oxygenated form was easily made by passage of ferrous Ctb down an aerated PD10 column. The species exhibited a Soret peak at 414 nm and α-β bands at 542 and 578 nm. A spectrum was scanned of whole *E. coli* cells over-expressing Ctb. The globin was found to be in the oxy form (data not shown; see Supporting Information Fig. S1).

Redox titration of Ctb

During reduction of Ctb it was observed that the globin was unusually slow in becoming fully reduced, taking approximately 15 min. This can be compared with leghemoglobin and horse heart myoglobin, both of which are fully reduced within a minute of adding dithionite. We postulated that the slow reduction of Ctb might be due to a low midpoint potential.

Controls were performed to ensure the reliability of the titrating system. The midpoint potential of horse heart cytochrome *c* was determined experimentally to be +261 mV. This compares favourably with literature values (+255 mV) (27). A blank titration was performed omitting Ctb to ensure that the spectral changes observed during titrations were due to Ctb and not to mediators. Titrations were always performed in the reductive direction, as the ferrous form was not reliably generated in significant quantities. The titration was taken from +200 mV to -400 mV to ensure full reduction of Ctb. Fig. 3 displays three titrations performed in both oxidising and reducing directions. The midpoint potential using the hydrogen electrode as reference is -33 mV.

Resonance Raman spectra

Fig. 4 shows the resonance Raman spectrum of the ferric derivative at pH values 7.0, 9.5 and 10.5. At neutral pH, ferric Ctb shows a typical mixture of six-coordinate high-spin and low-spin configurations as indicated by the ν_2 modes at 1563 and 1581 cm^{-1}, respectively, confirming that a water ligand is bound to the distal site of the heme. The intensity of the low-spin component, as reflected by the 1581 cm^{-1} band, develops as the pH increases, consistent with the de-protonation of the heme-bound water. The high-spin to low-spin transition is consistent with the optical absorption data, in which the intensities of bands at 542 and 582 nm bands increase with respect to those at 498 and 640 nm as the pH increases (data not shown; see Supporting Information Fig. S2).

The ferrous ligand-free form of Ctb exhibits a five-coordinate high-spin configuration as judged by the ν_3 and ν_4 modes at 1471 cm^{-1} and 1356 cm^{-1}, respectively. The $\nu_{Fe\text{-}His}$ mode, which is observable only in the five-coordinated deoxy species, was identified at 226 cm^{-1} (Fig. 5, top). It is identical to that of trHbN and trHbO, reflecting a strong iron-histidine bond.

In the high frequency region of the resonance Raman spectrum of the CO-derivative, ν_4 is located at 1372 cm^{-1} and ν_3 and ν_2 are located at 1498 and 1583 cm^{-1}, respectively (data not shown; see Supporting Information Fig. S3). The spectrum is characteristic of a ferrous six-coordinate heme protein. In the low frequency region, an isotope sensitive line at 514 cm^{-1} was observed (Fig. 5, bottom) that is shifted to 499 cm^{-1} in the $^{13}C^{18}O$ derivative, in accord with the predicted shift for a Fe–CO diatomic oscillator. In the isotope difference spectrum, all the heme-related modes are cancelled out to leave the two $\nu_{Fe\text{-}CO}$ lines appearing as a positive peak at 517 cm^{-1} for $^{12}C^{16}O$ and a negative peak at 494 cm^{-1} for $^{13}C^{18}O$ (Fig. 5, bottom). Likewise, a $\nu_{C\text{-}O}$ mode was identified at 1936 cm^{-1} on the basis of the isotope substitution experiment (data not shown).

An inverse correlation curve relating the frequencies of the Fe-CO stretching modes with those of the associated C-O stretching modes has been well established owing to the two resonance structures of the Fe-C-O moiety as shown below (28-30).

$$\underset{\text{(I)}}{\mathrm{LFeC} \equiv \mathrm{O}^{+}} \quad \leftrightarrow \quad \underset{\text{(II)}}{\mathrm{LFe{=}C{=}O}} \qquad \text{Eqn. 1}$$

Here, L represents the proximal iron ligand, a histidine in the case of Hbs. In general, a distal environment with positive polar residue(s) destabilizes the form (I), thereby strengthening the Fe-CO bond and concomitantly weakening the C-O bond. On the other hand, the identity of the proximal ligand L affects the electronic properties of the Fe-C-O moiety, such that the curve for imidazole / histidine coordinated species is distinct from that of thiolate coordinated species and that of the five-coordinate CO adduct. The CO-bound form of Ctb falls on the imidazole / histidine correlation curve (Fig. 6), confirming the assignment of the proximal ligand as a histidine.

On the imidazole / histidine correlation curve, the data points for the peroxidases typically locate at the higher left corner of the correlation line because of their polar distal environment. On the other hand, those of mammalian globins in general locate at the lower right corner of the correlation line because of the much more hydrophobic distal environment. In Hmp, two conformations were observed. One locates in the Mb region and the other locates in the peroxidase region, indicating that the distal pocket of Hmp is flexible and fluctuates between an open and a closed conformation. In the closed conformation, the heme-bound CO is stabilized by a H-bonding interaction involving the distal B10 Tyr and/or E7 Gln; this interaction is absent in the open conformation (31).

In vitro examination of Ctb

In preliminary experiments, supernatant fractions of cell extracts (i.e. with membranes centrifuged out) from *E. coli* over-expressing Ctb displayed double the O_2 consumption of control supernatants (L. M. Wainwright and R. K. Poole, unpublished). To test whether oxygen consumption could be demonstrated for the purified protein, as with Mb in the presence of methylene blue, NADH and cytochrome *c* reductase (32) or with Hmp (33), we used ascorbate (0.5 mM) or NADH (0.5 mM) as electron donors and phenazine methosulfate (PMS, 7 μM) as a redox mediator. However, no O_2 consumption by Ctb alone was observed. Reduction of Ctb was also sought spectrophotometrically. To pure Ctb (100 μg) in 50 mM Tris HCl pH 7.0 in an anaerobic glass cuvette were added several redox mediators (PMS, phenazine ethosulfate and methylene blue, 7 to 21 μM, final concentrations) with reductant (0. 5 mM ascorbate or NADH) and cytochrome c reductase (2.7 mg/ml). The spectrum was scanned against a buffer blank for approximately 30 min after addition of mediator and reductant. No reduction of Ctb could be demonstrated by these methods but addition of Na dithionite reduced the protein.

DISCUSSION

Significant advances have been made from crystallographic studies of purified trHbs, complemented by spectroscopic tools, particularly resonance Raman spectroscopy. In combination with site-directed mutagenesis, these methods have yielded important structural insights into some but not all of Wittenberg's groups.

Group I trHbs

The best-studied group I trHb is trHbN, which is expressed in stationary phase cultures of *M. tuberculosis* (34). The B10, E7, E10, E11 and E14 positions are occupied by Tyr, Leu, Lys, Gln and Phe respectively (reviewed in (13)). The importance of TyrB10 in stabilising heme-bound ligands is well established for several trHbs, including trHbN: mutation to Leu disrupts the H-bonding network and increases the O_2 off-rate by 200-fold (34). TrHbN displays $\nu_{Fe\text{-}CO}$ modes at 534 and 500 cm^{-1}, and matching $\nu_{C\text{-}O}$ modes at 1936 and 1960 cm^{-1} respectively (26), indicating that it has an Hmp-like equilibrium structure with fluctuating open

and closed conformations (13,26,31). The ferrous ligand-free derivative of trHbN has a five-coordinate configuration and the $\nu_{Fe\text{-}His}$ mode is at 226 cm^{-1} (26). Detailed studies on three other group I trHbs – trHbC from the green alga *Chlamydomonas eugametos*, trHbS from the cyanobacterium *Synechocystis*, and trHbP from the flagellate protozoan *Paramecium caudatum* – have been recently reviewed elsewhere (13).

Group II trHbs

An example of group II is provided by trHbO of *M. tuberculosis*, the second trHb in this bacterium. The most striking feature is the CD1 residue, which is not Phe as in almost all globins studied to date, but Tyr-36 (35). Furthermore, in the dodecameric crystalline state, the B10 Tyr is covalently bonded to the CD1 Tyr in six of the subunits, whilst in the remaining six the residue side chains are in intimate contact but without the covalent linkage (15). This unique CD1/B10 pair creates a rigid distal environment for heme-bound ligands. The $\nu_{Fe\text{-}His}$ mode is at 226 cm^{-1} (36). Unlike trHbN the CO derivative shows only one $\nu_{Fe\text{-}CO}$ mode at 525 cm^{-1}, which is assigned to a closed conformation (35).

Group III trHbs

Ctb, subject of this paper, is the first group III trHb to be described in detail. The optical spectra of purified Ctb closely resemble those of hemoglobins generally. The absorbance of the ferric Soret band is a few nm higher than is typical, but this is not significant. It is interesting that Ctb purifies predominantly in the ferrous-oxy form (Fig. 2, S1). Indeed, it would appear that oxygen binds to Ctb tightly, since even under anaerobic conditions the oxy form remains stable for at least a couple of hours. The tight binding of oxygen requires that the protein be deoxygenated prior to oxidation. The Fe-His stretching frequency of Ctb (226 cm^{-1} shown in Fig. 5) is similar to results obtained for other trHbs, lying between 220 and 232 cm^{-1} (13,25, 34,35,37). In mammalian Hb or Mb, the imidazole ring of the proximal histidine is in an eclipsed orientation with respect to the pyrrole nitrogen atoms of the porphyrin, in contrast to a staggered orientation in the trHbs (36). Consequently the proximal histidine is repelled from the porphyrin ring and results in a weakened proximal iron-histidine bond. This attenuation is manifested by the lower $\nu_{Fe\text{-}His}$ mode at ~214-220 cm^{-1} (38). On the other hand, the Fe-His mode of Hmp, the *E. coli* flavoHb, at 244 cm^{-1} is significantly larger than that of Ctb due to a H-bonding interaction between the proximal histidine and a nearby glutamate residue (13). The H-bond pulls the proton away from the histidine, giving it an imidazolate character. Similar large values of $\nu_{Fe\text{-}His}$ are found in peroxidases (240-260 cm^{-1}), where the histidine ligand also exhibits imidazolate character (31). This H-bonding interaction is not present in any of the trHbs with known structures, consistent with their relatively lower $\nu_{Fe\text{-}His}$. Taken together, these observations suggest that the proximal histidine ligand of Ctb has neutral character and has its imidazole ring in a staggered position with respect to the pyrrole nitrogen atoms of the porphyrin ring (13,25,31,34-38).

Ferrous Ctb under neutral conditions is five-coordinate and high-spin. This trait is displayed in a number of Hbs including trHbs found in *M. tuberculosis* (26,35), *Chlamydomonas* (25), *Paramecium* (37) and the flavoHb Hmp of *E. coli* (31). Only the trHb found in *Synechocystis* is six-coordinate and low-spin when reduced (39).

The Raman characteristics of the CO derivative (Fig. 5 and Fig. 6) show Ctb to have an atypical $\nu_{Fe\text{-}CO}$ stretching mode at 514 cm^{-1}, compared to the other truncated hemoglobins that have been characterized so far (13,26,31). The TyrB10, HisE7 and the TrpG8 in Ctb are highly conserved in the group III trHbs, suggesting ligand stabilisation roles of these residues in Ctb. The situation in Ctb is different from that in the trHbs of *Chlamydomonas* (25), *Paramecium* (37) and *Synechocystis* (39). In these three globins the stretching mode of the Fe-CO bond is

comparatively low at ~490 cm^{-1}. This is due to the open nature of the heme pocket, resulting in very little polar interaction of CO with the surrounding residues (13,37).

Functions of Ctb and other trHbs

Relatively little functional information is available on the various trHbs so that correlation between the proposed classification and function must remain tenuous. The fact that globins from different groups may coexist in the same organism, as in *C. jejuni* and *M. tuberculosis*, suggests that members of these subgroups are not functionally redundant. Indeed, *Mycobacterium avium* contains three trHbs, one from each subgroup. Lending support to this notion is the fact that the two trHbs of *M. tuberculosis* appear to have distinct functions: trHbN (group I) has been implicated in performing NO/O_2 chemistry and actively detoxifies NO yielding nitrate (40-42) whereas trHbO (group II) may play a role in oxygen transfer (18). Although the very high oxygen affinities of trHbO (43) and of the *Bacillus subtilis* group II trHb (44) appear inconsistent with intracellular oxygen management, recent data reveal the ability of this globin to bind phospholipids membranes with weak affinity for the terminal oxidase, cytochrome *bo*', of *E. coli* (45). Notwithstanding the uncertainty regarding trHbO (group II) function, the *M. leprae* GlbO in group II has been implicated in NO scavenging (46).

At present it seems premature to assign distinct functions to trHb groups I, II and III. The ancestor of contemporary globins, emerging perhaps 4,000 Mya, may have been trHb-like or like current single-domain (3/3) globins (1). It seems likely that such an ancestor evolved to deal with various diatomic ligands (O_2, NO, CO), and that contemporary trHbs preserve this ancient diversity of function, even within the somewhat arbitrary current classification. As for other trHbs, the function of Ctb is ambiguous. On the one hand, a role in oxygen metabolism is indicated by the growth phenotypes of a *ctb* mutant (19) and the effects of this deletion on the kinetics of oxidase-catalysed respiration. The finding that Ctb is oxygenated in whole *E. coli* cells indicates that the high affinity of the oxidases for O_2 (47,48) presents no obstruction to Ctb binding O_2 *in vivo*. This parallel with Vgb and also the similarity of the Ctb Raman data to that for trHbO leads us to hypothesise a role for Ctb in the facilitation of O_2 transfer to the terminal oxidases. The local O_2 concentration of the host environment of *C. jejuni* is most likely to be lower than is ideal for growth of the bacterium. Thus, *C. jejuni* may benefit from possessing an intracellular O_2-concentrating mechanism. However, when *C. jejuni* transfers between hosts, the bacterium will be exposed to significantly higher O_2 levels than those at which it can grow. A mechanism whereby excess O_2 is detoxified might appear beneficial. However, although *C. jejuni* possesses an iron superoxide dismutase encoded by *sodB* (49) that would protect against superoxide formation, the stability of the oxyferrous form argues against a reductive detoxification mechanism.

On the other hand, Cgb accumulation is increased on exposure to *S*-nitrosoglutathione (10) and transcriptional regulation of the *ctb* gene is mediated in response to nitrosative stress by NssR, a member of the Crp-Fnr superfamily (10). However, a *ctb* mutant is not hypersensitive to a range of nitrosative stress-inducing reagents (19). If Ctb were to be involved indirectly in NO detoxification it may, like Hmp, require reduction for sustained NO reductase or "oxygenase" (denitrosylase) activity. With a mid-point potential of −33 mV, Ctb appears capable of accepting electrons from NAD(P)H (-320 mV) and so an enzymatic activity of Ctb within the cell is not precluded but we were unable to reduce Ctb *in vitro* except with dithionite. Ctb may require a specific reductase to feed electrons to the heme iron *in vivo*. Indeed, Frey *et al.* (50) could not demonstrate NO consumption activity from *E. coli* over-expressing Cgb, probably because *E. coli* does not contain an appropriate reductase. The redox potential of Ctb is low when compared to other Hbs; Mbs from sperm whale, *Aplysia limacina* and Hb from *Chironomus thummi* have potentials of +50 mV, +150 mV and +120 mV respectively (51).

The Hb found in *Lumbricus terrestris* (earthworm) has a midpoint potential of +73 mV (52). The bacterial single domain globin Vgb found in *Vitreoscilla* purifies as a dimer, its two hemes having potentials of +118 and −122 mV (53). Further speculation concerning the function of Ctb is, of necessity, limited by the data available.

Conclusions

We report for the first time a detailed characterization of a group III trHb, *C. jejuni* Ctb. Although optical spectra of ferric, ferrous, O_2- and CO-bound forms resemble those of other hemoglobins, resonance Raman analysis shows Ctb to have an atypical $\nu_{Fe\text{-}CO}$ stretching mode at 514 cm^{-1}, compared to the other truncated hemoglobins that have been characterized so far. This implies unique roles in ligand stabilisation for TyrB10, HisE7 and TrpG8, residues highly conserved within group III truncated hemoglobins.

Supplementary Material

Refer to Web version on PubMed Central for supplementary material.

Acknowledgements

We thank Guanghui Wu and Karen Elvers for helpful discussions.

References

1. Vinogradov SN, Hoogewijs D, Bailly X, Arredondo-Peter R, Guertin M, Gough J, Dewilde S, Moens L, Vanfleteren JR. Three globin lineages belonging to two structural classes in genomes from the three kingdoms of life. Proc Natl Acad Sci U S A 2005;102:11385–9. [PubMed: 16061809]
2. Wu G, Wainwright LM, Poole RK. Microbial globins. Adv Microb Physiol 2005;47:255–310. [PubMed: 14560666]
3. Membrillo-Hernández J, Coopamah MD, Anjum MF, Stevanin TM, Kelly A, Hughes MN, Poole RK. The flavohemoglobin of *Escherichia coli* confers resistance to a nitrosating agent, a “nitric oxide releaser,” and paraquat and is essential for transcriptional responses to oxidative stress. J Biol Chem 1999;274:748–54. [PubMed: 9873011]
4. Crawford MJ, Goldberg DE. Role for the *Salmonella* flavohemoglobin in protection from nitric oxide. J Biol Chem 1998;273:12543–7. [PubMed: 9575213]
5. Liu LM, Zeng M, Hausladen A, Heitman J, Stamler JS. Protection from nitrosative stress by yeast flavohemoglobin. Proc Natl Acad Sci U S A 2000;97:4672–6. [PubMed: 10758168]
6. Poole RK, Hughes MN. New functions for the ancient globin family: bacterial responses to nitric oxide and nitrosative stress. Mol Microbiol 2000;36:775–83. [PubMed: 10844666]
7. Gardner PR, Gardner AM, Brashear WT, Suzuki T, Hvitved AN, Setchell KDR, Olson JS. Hemoglobins dioxygenate nitric oxide with high fidelity. J Inorg Biochem. 2006in the press
8. Park KW, Kim KJ, Howard AJ, Stark BC, Webster DA. *Vitreoscilla* hemoglobin binds to subunit I of cytochrome *bo* ubiquinol oxidases. J Biol Chem 2002;277:33334–7. [PubMed: 12080058]
9. Elvers KT, Wu G, Gilberthorpe NJ, Poole RK, Park SF. Role of an inducible single-domain hemoglobin in mediating resistance to nitric oxide and nitrosative stress in *Campylobacter jejuni* and *Campylobacter coli*. J Bacteriol 2004;186:5332–41. [PubMed: 15292134]
10. Elvers KT, Turner SM, Wainwright LM, Marsden G, Hinds J, Cole JA, Poole RK, Penn CW, Park SF. NssR, a member of the Crp-Fnr superfamily from *Campylobacter jejuni*, regulates a nitrosative stress-responsive regulon that includes both a single-domain and a truncated haemoglobin. Mol Microbiol 2005;57:735–50. [PubMed: 16045618]
11. Pesce A, Couture M, Dewilde S, Guertin M, Yamauchi K, Ascenzi P, Moens L, Bolognesi M. A novel two-over-two alpha-helical sandwich fold is characteristic of the truncated hemoglobin family. EMBO J 2000;19:2424–34. [PubMed: 10835341]

12. Wittenberg JB, Bolognesi M, Wittenberg BA, Guertin M. Truncated hemoglobins: A new family of hemoglobins widely distributed in bacteria, unicellular eukaryotes, and plants. J Biol Chem 2002;277:871–4. [PubMed: 11696555]

13. Egawa T, Yeh S-R. Structural and functional properties of hemoglobins from unicellular organisms as revealed by resonance Raman spectroscopy. J Inorg Biochem 2005;99:72–96. [PubMed: 15598493]

14. Milani M, Pesce A, Ouellet Y, Ascenzi P, Guertin M, Bolognesi M. *Mycobacterium tuberculosis* hemoglobin N displays a protein tunnel suited for O_2 diffusion to the heme. EMBO J 2001;20:3902–9. [PubMed: 11483493]

15. Milani M, Savard PY, Ouellet H, Ascenzi P, Guertin M, Bolognesi M. A TyrCD1/TrpG8 hydrogen bond network and a TyrB10-TyrCD1 covalent link shape the heme distal site of *Mycobacterium tuberculosis* hemoglobin O. Proc Natl Acad Sci U S A 2003;100:5766–71. [PubMed: 12719529]

16. Hoy JA, Kundu S, Trent JT, Ramaswamy S, Hargrove MS. The crystal structure of *Synechocystis* hemoglobin with a covalent heme linkage. J Biol Chem 2004;279:16535–42. [PubMed: 14736872]

17. Milani M, Pesce A, Bolognesi M, Ascenzi P. Truncated hemoglobins: trimming the classical 'three-over-three' globin fold to a minimal size. Biochemistry and Molecular Biology Education 2001;29:123–5.

18. Pathania R, Navani NK, Rajomohan G, Dikshit KL. *Mycobacterium tuberculosis* hemoglobin HbO associates with membranes and stimulates cellular respiration of recombinant *Escherichia coli*. J Biol Chem 2002;277:15293–302. [PubMed: 11796724]

19. Wainwright LM, Elvers KT, Park SF, Poole RK. A truncated haemoglobin implicated in oxygen metabolism by the microaerophilic food-borne pathogen *Campylobacter jejuni*. Microbiology-(UK) 2005;151:4079–91.

20. Friedman, CR.; Neimann, J.; Wegener, HC.; Tauxe, RV. Campylobacter. 2. Nachamkin, I.; Blaser, MJ., editors. ASM Press; Washington, DC: 2000. p. 121-38.

21. Pitcher DG, Saunders NA, Owen RJ. Rapid extraction of bacterial genomic DNA with guanidium thiocyanate. Lett Appl Microbiol 1989;8:151–6.

22. Inoue H, Nojima N, Okayama H. High efficiency transformation of *Escherichia coli* with plasmids. Gene 1990;96:23–8. [PubMed: 2265755]

23. Kalnenieks U, Galinina N, Bringer-Meyer S, Poole RK. Membrane D-lactate oxidase in *Zymomonas mobilis*: evidence for a branched respiratory chain. FEMS Microbiol Lett 1998;168:91–7. [PubMed: 9812368]

24. Dutton PL. Redox potentiometry: determination of midpoint potentials of oxidation-reduction components of biological electron-transfer systems. Meth Enzymol 1978;54:411–35. [PubMed: 732578]

25. Couture M, Das TK, Lee HC, Peisach J, Rousseau DL, Wittenberg BA, Wittenberg JB, Guertin M. *Chlamydomonas* chloroplast ferrous hemoglobin - Heme pocket structure and reactions with ligands. J Biol Chem 1999;274:6898–910. [PubMed: 10066743]

26. Yeh SR, Couture M, Ouellet Y, Guertin M, Rousseau DL. A cooperative oxygen finding hemoglobin from *Mycobacterium tuberculosis* - Stabilization of heme ligands by a distal tyrosine residue. J Biol Chem 2000;275:1679–84. [PubMed: 10636862]

27. Lemberg, R.; Barrett, J. Cytochromes. Academic Press; London: 1973.

28. Li X-Y, Spiro TG. Is bound CO linear or bent in heme proteins? Evidence from resonance Raman and infrared spectroscopic data. J Am Chem Soc 1988;110:6024–33.

29. Ray GB, Li X-Y, Ibers JA, Sessler JL, Spiro TG. How far can proteins bend the FeCO unit? Distal polar and steric effects in heme proteins and models. J Am Chem Soc 1994;116:162–76.

30. Vogel KM, Kozlowski PM, Zgierski MZ, Spiro TG. Role of the axial ligand in heme-CO backbonding; DFT analysis of vibrational data. Inorganica Chimica Acta 2000;297:11–7.

31. Mukai M, Mills CE, Poole RK, Yeh SR. Flavohemoglobin, a globin with a peroxidase-like catalytic site. J Biol Chem 2001;276:7272–7. [PubMed: 11092893]

32. Antonini, E.; Brunori, M. Hemoglobin and myoglobin in their reactions with ligands. North-Holland Publishing; Amsterdam: 1971.

33. Poole RK, Ioannidis N, Orii Y. Reactions of the *Escherichia coli* flavohaemoglobin (Hmp) with oxygen and reduced nicotinamide adenine dinucleotide: evidence for oxygen switching of flavin

oxidoreduction and a mechanism for oxygen sensing. Proceedings of the Royal Society of London Series B - Biological Sciences 1994;255:251–8.

34. Couture M, Yeh SR, Wittenberg BA, Wittenberg JB, Ouellet Y, Rousseau DL, Guertin M. A cooperative oxygen-binding hemoglobin from *Mycobacterium tuberculosis*. Proc Natl Acad Sci U S A 1999;96:11223–8. [PubMed: 10500158]
35. Mukai M, Savard PY, Ouellet H, Guertin M, Yeh SR. Unique ligand-protein interactions in a new truncated hemoglobin from *Mycobacterium tuberculosis*. Biochemistry 2002;41:3897–905. [PubMed: 11900532]
36. Samuni A, Ouellet Y, Guertin M, Friedman JM, Yeh S-R. The absence of proximal strain in the truncated hemoglobins from *Mycobacterium tuberculosis*. J Am Chem Soc 2004;126:2682–3. [PubMed: 14995168]
37. Das TK, Weber RE, Dewilde S, Wittenberg JB, Wittenberg BA, Yamauchi K, VanHauwaert ML, Moens L, Rousseau DL. Ligand binding in the ferric and ferrous states of *Paramecium* hemoglobin. Biochemistry 2000;39:14330–40. [PubMed: 11087382]
38. Friedman JM, Scott TW, Stepnoski RA, Ikeda-Saito M, Yonetani T. The iron-proximal histidine linkage and protein control of oxygen binding in hemoglobin. A transient Raman study. J Biol Chem 1983;258:10564–72. [PubMed: 6885793]
39. Couture M, Das TK, Savard PY, Ouellet Y, Wittenberg JB, Wittenberg BA, Rousseau DL, Guertin M. Structural investigations of the hemoglobin of the cyanobacterium *Synechocystis* PCC6803 reveal a unique distal heme pocket. Eur J Biochem 2000;267:4770–80. [PubMed: 10903511]
40. Ouellett H, Ouellett Y, Richard C, Labarre M, Wittenberg B, Wittenberg J, Guertin M. Truncated hemoglobin HbN protects *Mycobacterium bovis* from nitric oxide. Proc Natl Acad Sci U S A 2002;99:5902–7. [PubMed: 11959913]
41. Mukai M, Ouellet Y, Ouellet H, Guertin M, Yeh SR. No binding induced conformational changes in a truncated hemoglobin from *Mycobacterium tuberculosis*. Biochemistry 2004;43:2764–70. [PubMed: 15005611]
42. Crespo A, Marti MA, Kalko SG, Morreale A, Orozco M, Gelpi JL, Luque FJ, Estrin DA. Theoretical study of the truncated hemoglobin HbN: Exploring the molecular basis of the NO detoxification mechanism. J Am Chem Soc 2005;127:4433–44. [PubMed: 15783226]
43. Ouellet H, Juszczak L, Dantsker D, Samuni U, Ouellet YH, Savard PY, Wittenberg JB, Wittenberg BA, Friedman JM, Guertin M. Reactions of *Mycobacterium tuberculosis* truncated hemoglobin O with ligands reveal a novel ligand-inclusive hydrogen bond network. Biochemistry 2003;42:5764–74. [PubMed: 12741834]
44. Giangiacomo L, Ilari A, Boffi A, Morea V, Chiancone E. The truncated oxygen-avid hemoglobin from *Bacillus subtilis* - X-ray structure and ligand binding properties. J Biol Chem 2005;280:9192–202. [PubMed: 15590662]
45. Liu C, He Y, Chang ZY. Truncated hemoglobin *o* of *Mycobacterium tuberculosis*: the oligomeric state change and the interaction with membrane components. Biochem Biophys Res Commun 2004;316:1163–72. [PubMed: 15044107]
46. Ascenzi P, Bocedi A, Bolognesi M, Fabozzi G, Milani M, Visca P. Nitric oxide scavenging by *Mycobacterium leprae* GlbO involves the formation of the ferric heme-bound peroxynitrite intermediate. Biochem Biophys Res Commun 2006;339:450–6. [PubMed: 16307730]
47. D'mello R, Hill S, Poole RK. The oxygen affinity of cytochrome *bo'* in *Escherichia coli* determined by the deoxygenation of oxyleghemoglobin and oxymyoglobin: K_m values for oxygen are in the submicromolar range. J Bacteriol 1995;177:867–70. [PubMed: 7836332]
48. D'mello R, Hill S, Poole RK. The cytochrome *bd* quinol oxidase in *Escherichia coli* has an extremely high oxygen affinity and two oxygen-binding haems: implications for regulation of activity *in vivo* by oxygen inhibition. Microbiology 1996;142:755–63. [PubMed: 8936304]
49. Pesci EC, Cottle DL, Pickett CL. Genetic, enzymatic and pathogenic studies of the iron superoxide dismutase of *Campylobacter jejuni*. Infect Immun 1994;62:2687–94. [PubMed: 8005660]
50. Frey AD, Farres J, Bollinger CJT, Kallio PT. Bacterial hemoglobins and flavohemoglobins for alleviation of nitrosative stress in *Escherichia coli*. Appl Environ Microbiol 2002;68:4835–40. [PubMed: 12324328]

51. Brunori M, Saggese U, Rotilio GC, Antonini E, Wyman J. Redox equilibrium of sperm-whale myoglobin, *Aplysia* myoglobin and *Chironomus thummi* hemoglobin. Biochemistry 1971;10:1604–9. [PubMed: 5580671]

52. Dorman SC, Harrington JP, Martin MS, Johnson TV. Determination of the formal reduction potential of *Lumbricus terrestris* hemoglobin using thin layer spectroelectrochemistry. J Inorg Biochem 2004;98:185–8. [PubMed: 14659648]

53. Tyree B, Webster DA. Electron-accepting properties of cytochrome *o* purified from *Vitreoscilla*. J Biol Chem 1978;253:7635–7. [PubMed: 701279]

Abbreviations

Ctb
: *Campylobacter* truncated hemoglobin

Hb
: hemoglobin

Mb
: myoglobin

MOPS
: morpholinopropanesulfonic acid

trHb
: truncated hemoglobin

Vgb
: *Vitreoscilla* hemoglobin

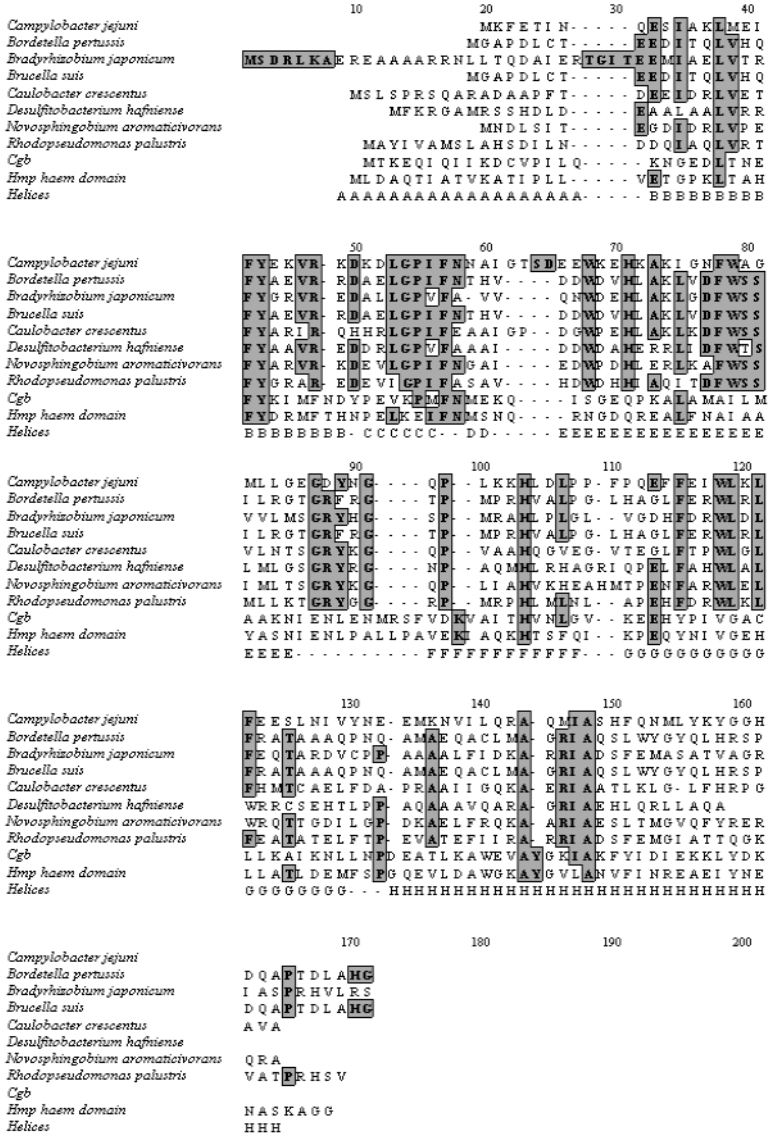

FIGURE 1.

Sequence alignment of *C. jejuni* trHb with various trHbs, Cgb and the Hmp heme domain. The sequence comparison was carried out using Clustal W. The top eight sequences are trHbs, followed by the non-truncated globin (Cgb) of *C. jejuni* and the N-terminal heme domain of *E. coli* flavohemoglobin (Hmp). The locations of the respective helices (A-H) are displayed in the bottom line below the aligned sequences. Conserved residues are shaded. Sequence data for various hemoglobins were obtained from TIGR.

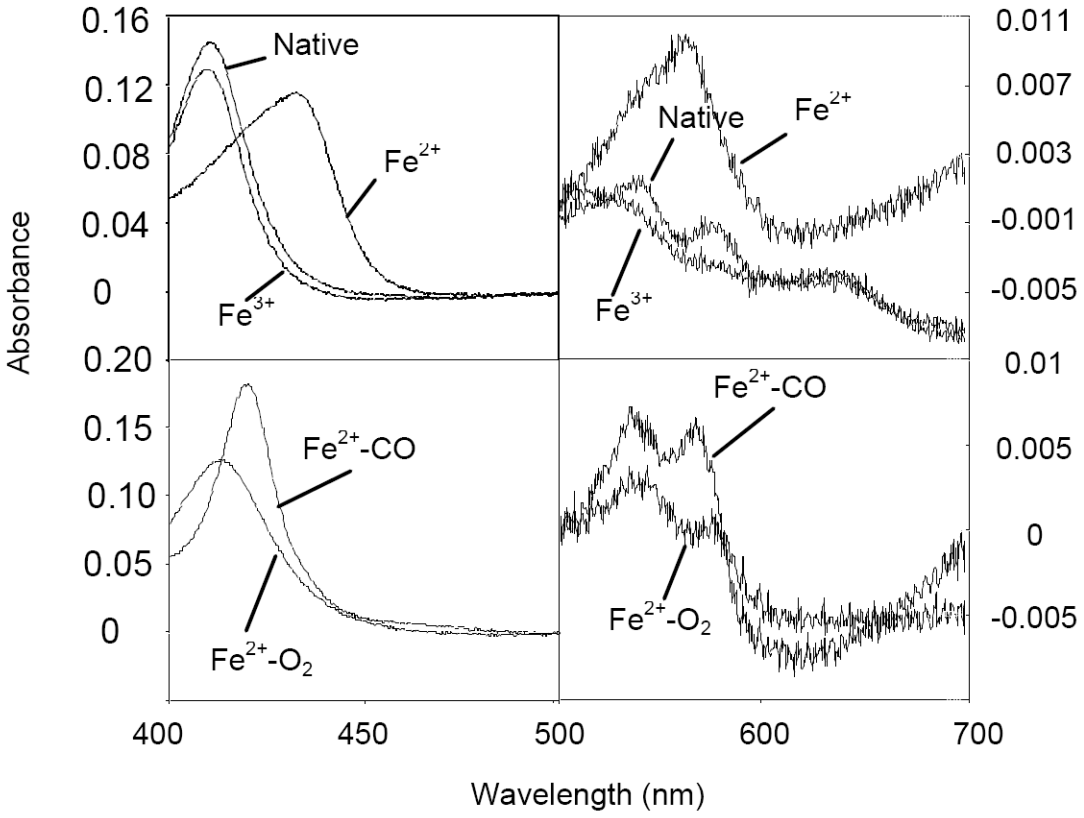

FIGURE 2.

Electronic absorbance spectra of pure Ctb. All spectra were scanned against a 50 mM Tris HCl pH 7.0 baseline and are normalised to heme concentration (0.001 nM). Native Ctb corresponds to the globin as it elutes from the gel filtration column (peak maxima at 411, 512, 542, 578 and 640 nm). The other forms of Ctb were generated as described in the text. Peak maxima are as follows. Fe^{2+}, 432 and 565 nm; Fe^{3+}, 410, 512, 542, 582 and 640 nm; Fe^{2+}-CO, 421, 538 and 569 nm; Fe^{2+}-O_2, 414, 542 and 578 nm.

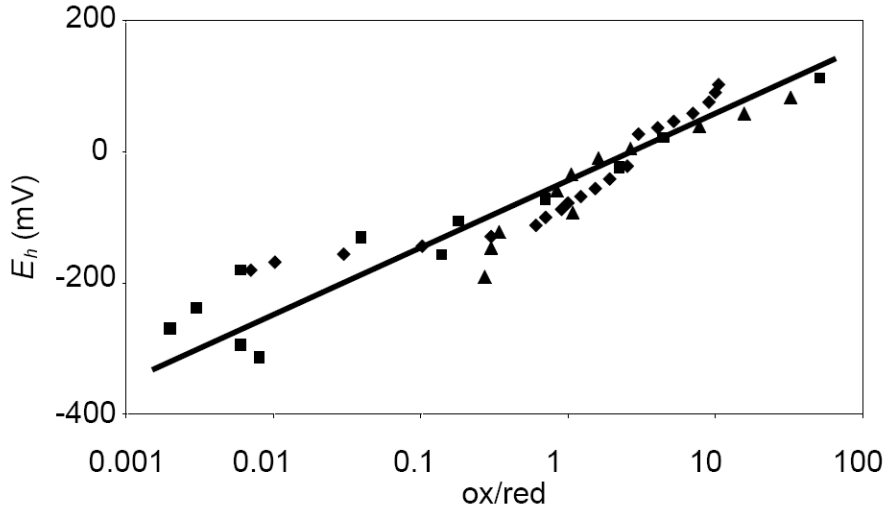

FIGURE 3.

Redox titration of Ctb. The electrochemical potential was plotted against % oxidised Ctb/ % reduced Ctb in a semilog arithmetic plot according to the Nernst equation. Reducing (diamonds, triangles) and oxidising (squares) titrations are shown. The line has been fitted to all three titrations ($R^2 = 0.83$).

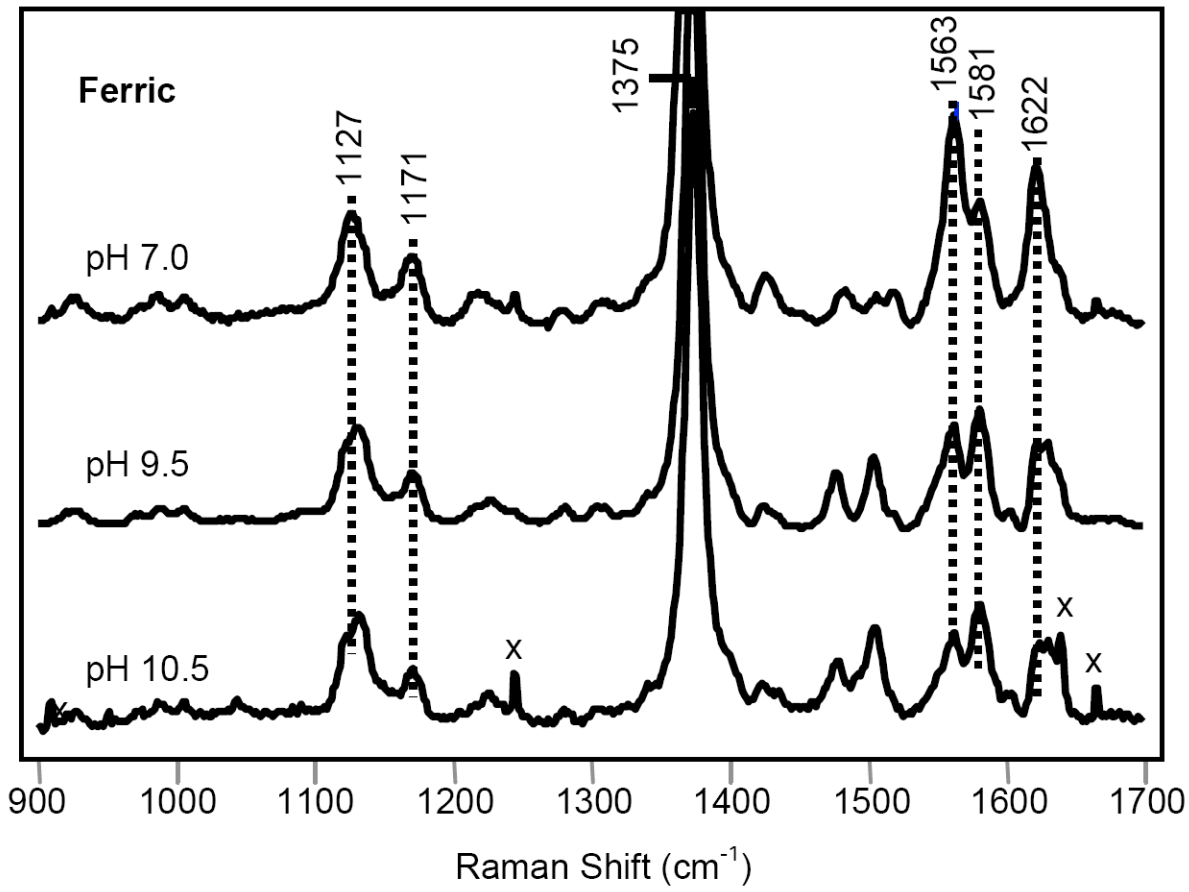

FIGURE 4.
Resonance Raman spectra of ferric Ctb. The Raman spectrum of the ferric form was obtained at pH 7.0, 9.5 and 10.5.

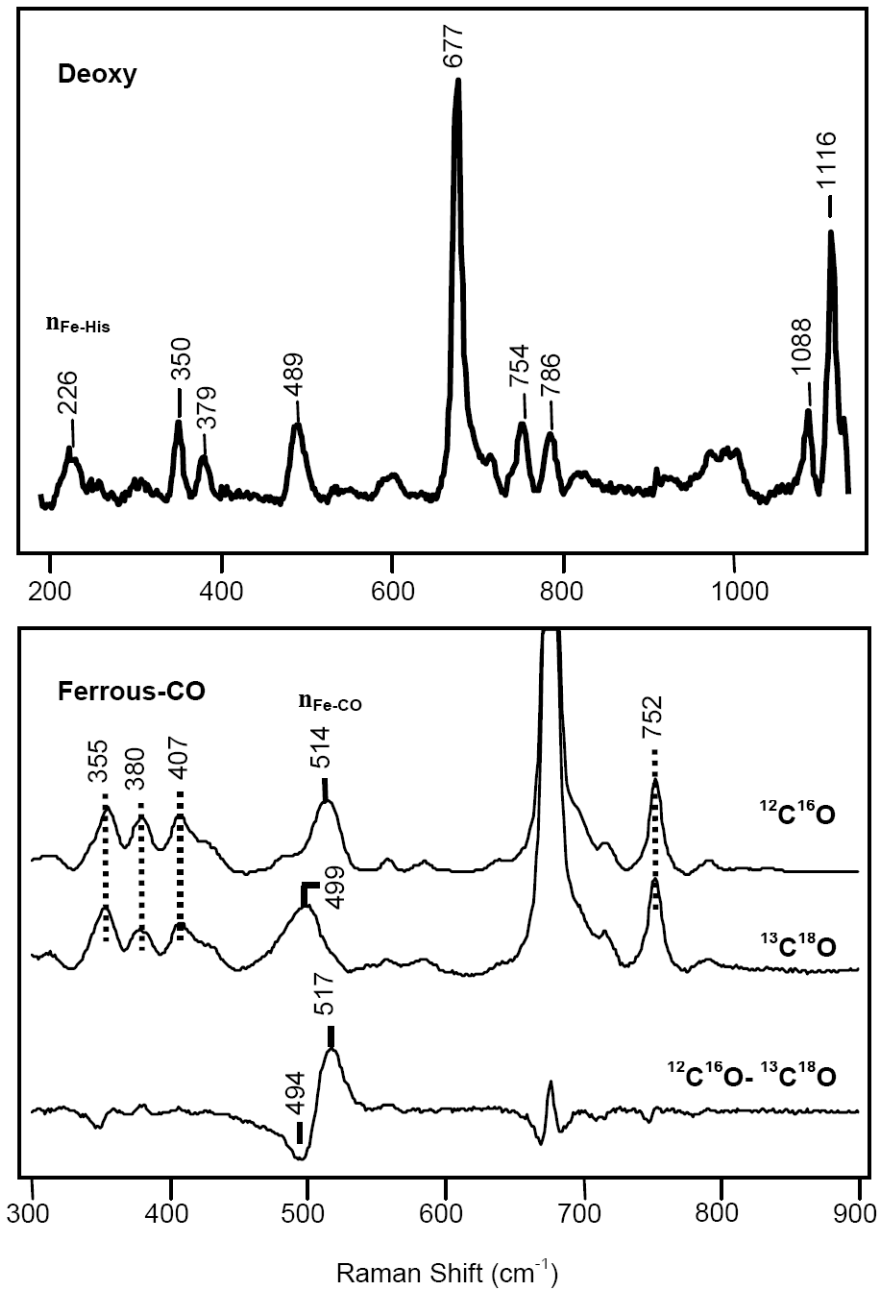

FIGURE 5.

Top: Resonance Raman spectra of deoxy and CO-bound derivatives of Ctb. The Raman spectra of the ferrous deoxy form (top) and the Fe^{2+}-CO form (bottom) of Ctb.

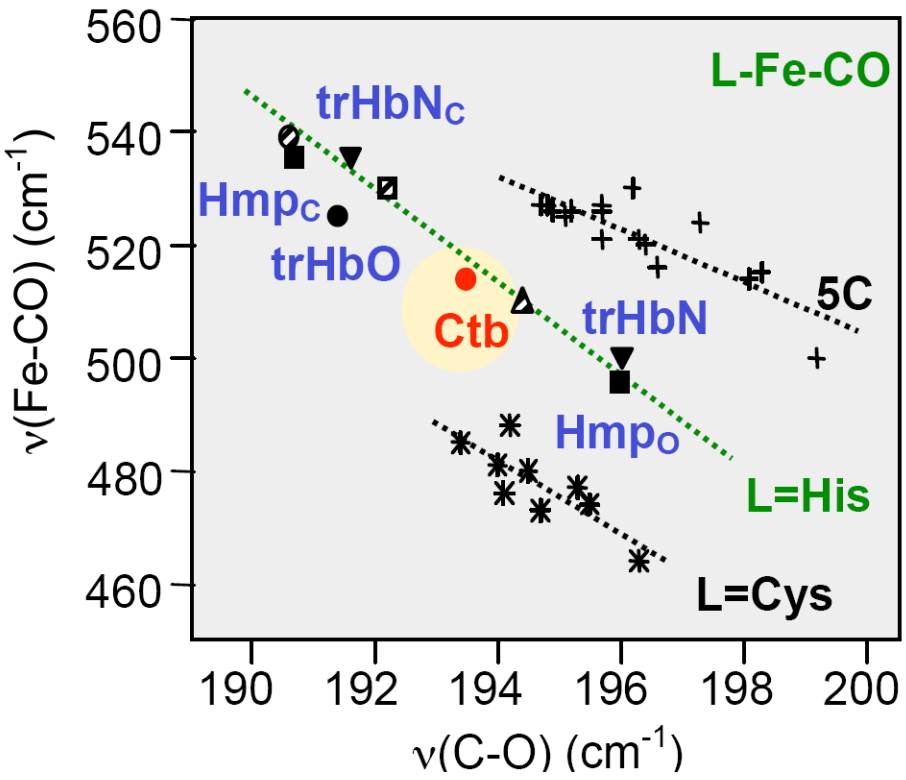

FIGURE 6.

Inverse correlation diagram of the Fe-CO stretching frequency *versus* the C-O stretching frequency of various heme proteins, and comparison with Ctb. The solid inverted triangles represent trHbN in closed ($trHbN_C$, upper) and open ($trHbN_O$, lower) conformations. Nearby, the solid squares represent Hmp in closed and open conformations. TrHbO is represented by the red, solid circle in the top left portion of the plot, and Ctb by the circle in the centre of the L=His line. The striped circle (extreme top left), striped square and striped triangle (middle) represent horseradish peroxidase, cytochrome *c* peroxidase and Mb, respectively. The L=Cys line corresponds to those proteins where the proximal ligand to the heme is the thiolate side chain of cysteine, the L=His line corresponds to those proteins where the proximal ligand is the imidazole/imidazolate side chain of histidine, and the 5C line corresponds to those proteins where the CO-bound form is penta-coordinate.